NASA Technical Paper 2779

1988

Life Prediction of Thermomechanical Fatigue Using Total Strain Version of Strainrange Partitioning (SRP)

A Proposal

James F. Saltsman
and Gary R. Halford

Lewis Research Center
Cleveland, Ohio

National Aeronautics
and Space Administration

Scientific and Technical Information Division

Summary

A method is proposed (without experimental verification) for extending the total strain version of Strainrange Partitioning (TS-SRP) to predict the lives of thermomechanical fatigue (TMF) cycles. The principal feature of TS-SRP is the determination of the time-temperature-waveshape dependent elastic strainrange versus life lines that are added subsequently to the classical inelastic strainrange versus life lines to form the total strainrange versus life relations. The procedure is based on a derived relation between "failure" and "flow" behavior. "Failure" behavior is represented by conventional SRP inelastic strainrange versus cyclic life relations, while "flow" behavior is captured in terms of the cyclic stress-strain response characteristics. Stress-strain response is calculated from simple equations developed from approximations to more complex cyclic constitutive models. For application to TMF life prediction, a new testing technique, bithermal cycling, is proposed as a means for generating the inelastic strainrange versus life relations. Flow relations for use in predicting TMF lives would normally be obtained from approximations to complex thermomechanical constitutive models. Bithermal flow testing is also proposed as an alternative to thermomechanical flow testing at low strainranges where the hysteresis loop is difficult to analyze. For the current paper, cyclic stress-strain response is calculated for the alloy 2-1/4Cr-1Mo steel in the post-weld, heat-treated condition for both thermomechanical and bithermal cycles and for a variety of strainranges and hold times. Bithermal failure behavior data are currently unavailable.

Introduction

Strainrange Partitioning (SRP) (ref. 1) was originally formulated on an inelastic strainrange versus cyclic life basis for isothermal conditions. The approach has worked well in the high-strain, low-life regime where the inelastic strains are large enough to be determined accurately by analytical and experimental methods.

To extend the method into the low-strain, long-life regime where the inelastic strains are small and difficult to determine, it was necessary to consider the total rather than just the inelastic strainrange. Formulating SRP on a total strain basis (TS-SRP) (refs. 2 and 3) required the determination of both the inelastic and the elastic strainrange versus cyclic life relations for cycles involving creep strain. The elastic strainrange versus life relations for cycles involving creep are influenced significantly by temperature, hold time, waveshape (CC, CP, and PC), and how creep is introduced into the cycle (stress hold, strain hold, slow strain rate, etc.). To make the analysis tractable, we have assumed that the elastic life lines are displaced parallel to themselves and are parallel to the elastic life line for PP cycling. This means that for a given imposed cycle type at a specific temperature, the elastic line intercept (elastic strainrange at $N_f = 1$ cycle) is a function only of the time of the cycle. In the first version of TS-SRP (ref. 2), the elastic line intercept was determined by the use of an empirical equation with constants determined using data obtained from failure tests. Efforts to reduce testing requirements led to the development of an updated version of TS-SRP (ref. 3). This development was based on a derived relation between failure behavior (inelastic strainrange versus cyclic life) and flow behavior (cyclic stress-strain response) and greatly reduced the time and cost of characterizing the TS-SRP behavior of an alloy. Failure behavior is characterized readily in the high-strain, low-life regime where testing times are reasonable, and the critical flow behavior is characterized in the desired low-strain, long-life regime by cycling a specimen just long enough for the stress-strain hysteresis loop to approach stability. With this approach, the elastic line intercept can be established with a minimum of long-time testing.

Traditionally, thermomechanical fatigue[1] (TMF) resistance of materials has been estimated by conducting isothermal fatigue tests at the expected maximum temperature in the TMF cycle, with effects of creep being determined by imposing hold periods at peak tensile or compressive strain. Computer-controlled testing equipment and techniques have recently been developed to the point where thermomechanical fatigue tests can be conducted routinely, so isothermal testing is no longer as justifiable. However, true TMF cycles become difficult to control, analyze, and interpret at low strainranges, and bithermal fatigue testing has been proposed (ref. 4) to avoid this difficulty.

[1]The term "thermomechanical fatigue" is used to indicate variable temperature fatigue in which the mechanical strain is imposed only by externally applied loads. Temperature gradients within the test volume are not permitted.

Existing methods for predicting TMF life of components in the low-strain regime are lacking in accuracy or generality. Thus, we have actively pursued development of a TMF life-prediction method that would overcome these deficiencies. As a starting point, we have selected the SRP method because of past successes. For example, the inelastic strain version of SRP has been successfully applied to a thermomechanical fatigue problem (ref. 5) at a strain level where the inelastic strainrange could be determined accurately and for which the life relations are temperature independent. Also, the TS–SRP version has been applied successfully to isothermal problems (refs. 2 and 3) where the inelastic strainrange cannot be determined accurately. These successes suggest that the total strain version has the potential to be extended to predict the lives of TMF cycles at low strainranges.

This report examines the extension of TS–SRP into the TMF regime by the use of a hypothetical example for the pressure vessel and piping steel alloy 2-1/4Cr-1Mo. The cyclic stress-strain-time, that is, flow response, has been determined for both thermomechanical and bithermal cycles using the Robinson flow model (ref. 6). Unfortunately, adequate TMF failure data for this alloy, especially in the low strain regime, are not available so we cannot verify the TS–SRP life predictions at this time. The characterization of an alloy by TS–SRP requires the determination of both failure and flow responses.

Symbols

A	general constant in empirical flow equations
A'	general constant in empirical flow equations
B	intercept of elastic strainrange versus life relation
C	intercept of inelastic strainrange versus life relation
C'	intercept of equivalent inelastic line for combined creep-fatigue cycles with parallel inelastic failure lines
C''	intercept of equivalent inelastic line for combined creep-fatigue cycles with nonparallel inelastic failure lines
CC	creep strain in tension, creep strain in compression
CP	creep strain in tension, plastic strain in compression
f	frequency
F	strain fraction
K	cyclic strain-hardening coefficient
N	number of cycles to failure
PC	plastic strain in tension, creep strain in compression
PP	plastic strain in tension, plastic strain in compression
R	mean stress correction term for nonisothermal fatigue
r	correlation coefficient
t	hold time per cycle
V	fatigue mean stress correction term; isothermal and nonisothermal
y	general dependent variable
Δ	range of variable
ϵ	strain
$\dot{\epsilon}$	strainrate
σ	stress
τ	period of one cycle

Subscripts:

amp	amplitude
bi	bithermal
c	compression
cc	creep strain in tension, creep strain in compression
cp	creep strain in tension, plastic strain in compression
el	elastic
eff	effective
fm	failure; mean stress condition
f_o	failure; zero mean stress condition
in	inelastic
ij	*pp, cc, pc, cp*
m	mean
max	maximum value
min	minimum value
pc	plastic strain in tension, creep strain in compression
pp	plastic strain in tension, plastic strain in compression
pre	predicted
t	tension or total strain
tm	thermomechanical
σ	stress

Superscripts:

b	time-independent power of cyclic life for elastic strainrange versus life relation
b'	time-dependent power of cyclic life for elastic strainrange versus life relation
c	power of cyclic life for inelastic strainrange versus life relations
c^*	power of cyclic life for inelastic strainrange versus life relations
m	general power of time in empirical flow equations
n	time-independent, cyclic strain-hardening exponent
n'	time-dependent, cyclic strain-hardening experiment
α	power on total strainrange in empirical flow equations

Cycle type (nonisothermal):

HRIP high-rate inphase cycle producing 100-percent PP strainrange

HROP high-rate out-of-phase cycle producing 100-percent PP strainrange

THIP tensile hold inphase cycle with hold period at maximum tensile strain producing CP and PP strainranges

CHOP compressive hold out-of-phase cycle with hold period at minimum compressive strain producing PC and PP strainranges

Analysis

In formulating TS-SRP for isothermal fatigue (refs. 2 and 3), we assumed that the inelastic and elastic strainrange versus life lines for creep-fatigue cycles are parallel to the corresponding lines for pure fatigue or PP cycles, as shown in figure 1. This is not an arbitrary assumption since our experience with several alloys suggests that this is reasonable behavior for isothermal conditions. Note that the frequency modified approach of Coffin (ref. 7) also uses parallel inelastic and elastic lines. We assume, in the absence of data for guidance, that this will also be the case for nonisothermal conditions.

Based on the above assumptions, a relationship between failure behavior and flow behavior can be established. Failure behavior is expressed by the equations for elastic and inelastic strainrange versus cyclic life:

$$\Delta\epsilon_{el} = B(N_{fo})^b \tag{1}$$

$$\Delta\epsilon_{in} = C'(N_{fo})^c \tag{2}$$

where

$$C' = \left[\sum F_{ij}(C_{ij})^{1/c}\right]^c \tag{3}$$

and

$$ij = pp,\ cc,\ pc,\ \text{or}\ cp$$

Equation (3) is derived from the interaction damage rule (IDR) of reference 8 and the four generic SRP inelastic strainrange—cyclic life relations for a theoretical zero mean stress condition. In the past the inelastic line intercepts for creep cycles (C_{pc}, C_{cp}, and C_{cc}) were taken to be independent of time. But recent developments (ref. 9) indicate that they may be time dependent at elevated temperatures, and procedures have been proposed for expressing the time dependencies analytically. The following development of the TMF life-prediction method based on TS-SRP will not explicitly consider the time dependency of the inelastic lines, although it could be added if needed.

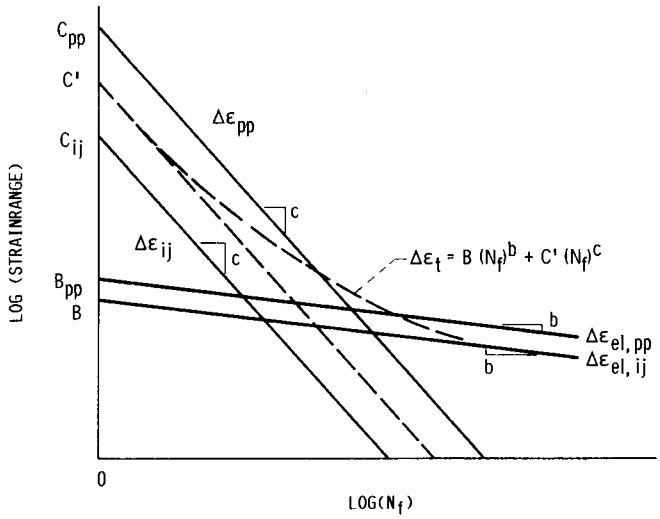

Figure 1.—Relation between total strainrange and life for nonisothermal creep-fatigue cycles. Inelastic line intercept C' is determined from equation (3) and elastic line intercept B is determined from equation (7).

The four generic SRP relations are

$$\Delta\epsilon_{in} = C_{ij}(N_{ij})^c \tag{4}$$

The IDR is written as follows:

$$\sum\left[\frac{F_{ij}}{N_{ij}}\right] = \frac{1}{N_{fo}} \tag{5}$$

where $\Sigma F_{ij} = 1.0$. Using equation (4) to solve for N_{ij} and substituting into equation (5), we obtain equation (3). Flow behavior is expressed by an equation relating elastic and inelastic strainranges:

$$\Delta\epsilon_{el} = K_{ij}(\Delta\epsilon_{in})^n \tag{6}$$

where $n = b/c$.

Based on the assumption that the inelastic and elastic failure lines for creep-fatigue cycles are parallel to the corresponding failure lines for PP cycles, it follows that the strain-hardening exponent n in equation (6) is a constant as shown in figure 2.

For isothermal conditions the strain-hardening coefficient K_{ij} is a function of temperature, hold time, how creep is introduced into the cycle (stress hold, strain hold, etc.), and the strainrate-hardening characteristics of the alloy. For nonisothermal conditions it is also a function of the maximum and minimum temperatures and the phase relation between strain and temperature.

The time-dependent behavior of the elastic strainrange-life relation for creep cycles is shown schematically in figure 3. Setting equation (1) equal to equation (6) and eliminating N_{fo}

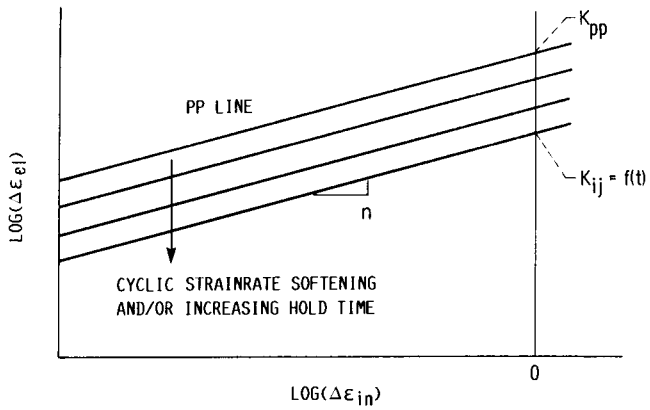

Figure 2.—Relation between inelastic and elastic strainranges for nonisothermal creep-fatigue cycles. Cyclic strain-hardening coefficient K_{ij} is a function of hold time, maximum and minimum cycle temperatures, phase relation between strain and temperature, and strainrate-hardening characteristics of an alloy.

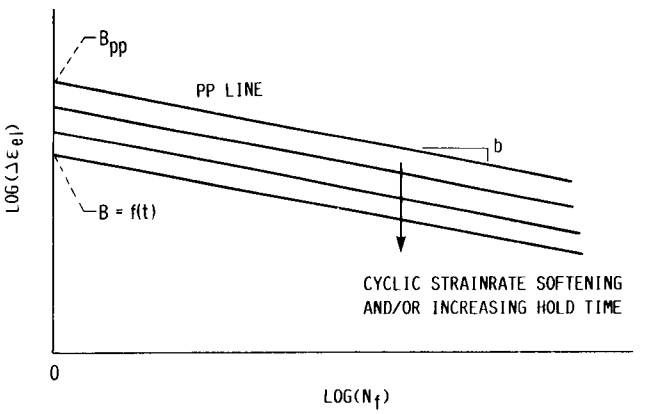

Figure 3.—Relation between elastic strainrange and life for nonisothermal creep-fatigue cycles. Variation in elastic line intercept is a function of hold time, maximum and minimum cycle temperatures, phase relation between strain and temperature, and strainrate-hardening characteristics of an alloy.

using equation (2), we obtain the following equation relating flow and failure behavior:

$$B = K_{ij}(C')^n \tag{7}$$

In this equation the inelastic line intercepts C_{ij} and the exponent c used to determine C' are considered to be failure terms. The strain fractions F_{ij}, the strength coefficient K_{ij}, and the strain-hardening exponent n are considered to be flow terms. Thus, the elastic line intercept B can be determined for a creep cycle from a combination of flow and failure data. Note that K_{ij} and F_{ij} will, in general, depend on waveform.

We are now in a position to establish a total strainrange versus life relation and thus predict life on a total strainrange basis. Note that the SRP inelastic strainrange versus life relations and the flow relations are determined for a specified minimum and maximum temperature and phase relationship between strain and temperature. The total strainrange is

$$\Delta\epsilon_t = \Delta\epsilon_{el} + \Delta\epsilon_{in} \tag{8}$$

From equations (1) and (2) we obtain

$$\Delta\epsilon_t = B(N_{fo})^b + C'(N_{fo})^c \tag{9}$$

A schematic plot of equation (9) is shown in figure 1. Note that the solution of this equation gives the cyclic life N_{fo} for a theoretical zero mean stress condition. The final step in a life prediction is to adjust the computed life to account for any mean stress effects that may be present.

A method for accounting for mean stress effects on life for isothermal conditions has been proposed in reference 10;

$$(N_{fm})^b = (N_{fo})^b - V_{eff} \tag{10}$$

where N_{fm} and N_{fo} are the lives with and without mean stress, respectively, and V_{eff} is the effective mean stress correction term. For isothermal fatigue, V_{eff} is determined by the following equation:

$$V_{eff} = V_\sigma \exp\left[-70\left(\frac{\Delta\epsilon_{in}}{\Delta\epsilon_{el}}\right)^2\right] \tag{11}$$

where $V_\sigma = \sigma_m/\sigma_{amp}$. Note that this method of correcting for the mean stress effect on cyclic life was developed for a specific nickel-base alloy and may not apply to other alloys or even to other nickel-base alloys. The analyst must determine that the mean stress correction equation used is applicable to the alloy of interest.

For TMF an alternate definition of V_{eff} is in order since a mean stress can naturally develop because of the temperature dependency of the yield strength in tension and compression. Hence, V_{eff} in equation (10) should be determined (ref. 11) by the following:

$$V_{eff} = \frac{1 + \dfrac{R_\sigma}{R_y}}{1 - \dfrac{R_\sigma}{R_y}} \tag{12}$$

where R_σ is equal to $\sigma_{min}/\sigma_{max}$ and R_y is the absolute value of the ratio of the compressive yield strength to the tensile yield strength at their respective maximum and minimum temperatures and strainrates in the TMF cycle. To date there is no direct experimental verification of this method for accounting for mean stress effects for nonisothermal fatigue.

To predict life on a total strainrange basis, it is necessary first to determine the PP inelastic and elastic lines and the desired SRP inelastic strainrange versus life relations experimentally. Note that these relations are to be established for a theoretical zero mean stress condition. Empirical estimation methods developed for isothermal fatigue, such as

the ductility-normalized SRP relations (ref. 12) are not recommended at this time as they have not been verified for application to TMF. Ideally, failure and flow behavior would be determined from TMF tests duplicating the cycles for which lives are to be predicted. However, this approach is impractical as it lacks generality of use. For example, if the cycle were to change, the entire data base would have to be regenerated at a doubling of cost and lead time. Further changes would in turn require further repetition of experiments. A more basic approach is thus required. While an isothermal approach would offer advantages in terms of costs because of the vast background of isothermal data bases, we do not, at this time, recommend doing so. This recommendation comes as a result of an indepth survey (ref. 11) comparing the TMF and isothermal fatigue resistances of many alloys. Only under special circumstances of temperature invariant deformation and cracking mechanisms could isothermal fatigue resistance be used to accurately predict TMF results.

At this stage of development of the TS–SRP approach, we recommend resorting to bithermal fatigue tests (ref. 4) to generate the experimental inelastic strainrange-life relations required by TS–SRP. Bithermal fatigue offers the simplicity of isothermal testing, yet it captures the first-order effects of inphase and out-of-phase TMF cycling. The bithermal tests should cover a sufficient temperature range to encompass the deformation and cracking mechanisms pertinent to the TMF cycles of interest. Determination of the critical temperature ranges for testing will require a rudimentary understanding of the metallurgical factors governing the deformation and cracking mechanisms. Thermomechanical flow tests would normally be conducted to properly characterize the stress-strain response, but bithermal flow tests could be conducted at the lower strainranges where the inelastic strains are small and it is difficult to analyze the thermomechanical hysteresis loops. The stress-strain response of the two types of cycles should be similar in this strain regime, and the bithermal cycle would be a good approximation to the thermomechanical cycle. The thermomechanical and bithermal cycles used in this report are shown in figure 4.

Techniques are described in reference 4 for determining PP life relations for inphase and out-of-phase bithermal cycles, CP inphase, and PC out-of-phase inelastic strainrange-life relations. Proposals for the determination of a CC bithermal life relation have not been discussed because of the exclusion of such a strainrange component in TMF cycles at small inelastic strainranges.

The strain-hardening coefficient K_{ij} and the strain fraction F_{ij} can be determined using an appropriate constitutive flow model for which the material constants are available. As an alternative, they could be determined by conducting flow tests for the creep-fatigue cycles of interest. Using these data, one can determine the necessary empirical correlations describing flow behavior. This latter approach is the most viable option at this time because reliable constitutive flow models in the low strain regime and the required material constants are not yet generally available. The procedures for determining the flow correlations are described in the following section.

The strainrange analysis presented above is based on the assumption that the inelastic and elastic versus life lines for creep-fatigue cycles are parallel to the corresponding lines for PP cycles. This may not always be a satisfactory assumption. (The case of nonparallel lines is discussed in the appendix.)

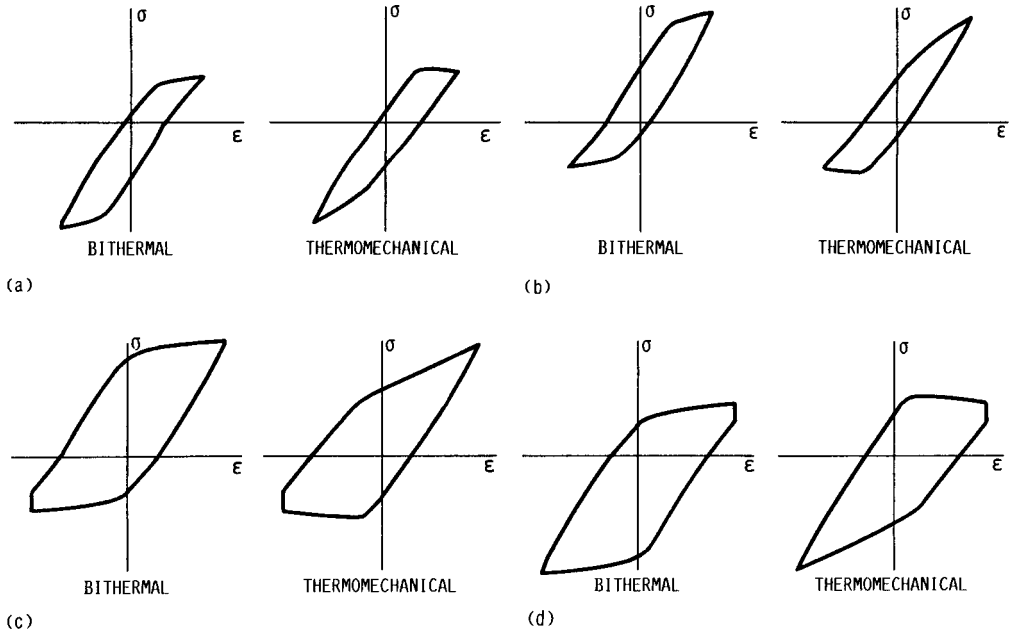

(a) PP cycle, inphase. (b) PP cycle, out-of-phase.
(c) PC cycle, out-of-phase. (d) CP cycle, inphase.

Figure 4.—Bithermal and TMF waveshapes used in this report.

Analysis Using Robinson Constitutive Model

The choice of a constitutive model for use with TS-SRP is somewhat arbitrary. We have selected the Robinson model (refs. 6 and 13) because it has been validated for TMF application (using the alloy 2-1/4Cr-1Mo steel in the post-weld, heat-treated condition). Using Robinson's model, we have obtained the simple power law correlation shown below. This same power law form was also used successfully to correlate isothermal flow data (ref. 3):

$$y = A(t)^m \tag{13}$$

where y is the dependent variable representing several different flow variables, as will be discussed shortly, and t is the hold time per cycle.

Generally, the intercept A (value of y at $t = 1$) is a function of total strainrange. The results obtained from the Robinson model for thermomechanical cycles and earlier results for isothermal cycles using the Walker model (refs. 3 and 13) show that the family of lines shown in figure 5 can be taken as parallel. Thus, the exponent on time m is assumed to be independent of total strainrange. By a process of trial and error, we determined that the intercept A can be correlated with total strainrange by another power law as shown in figure 6;

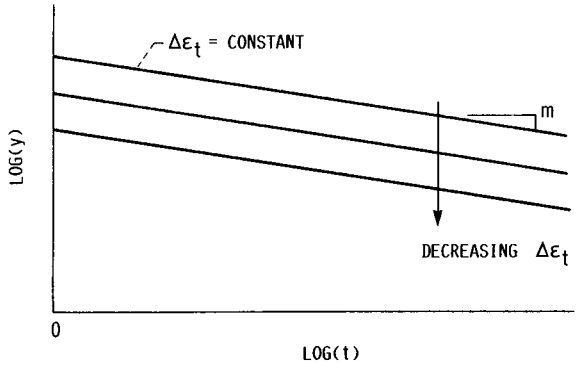

Figure 5.—Power law relation used to correlate flow data. Lines are parallel, and intercept A at $t = 1$ sec is a function of total strainrange.

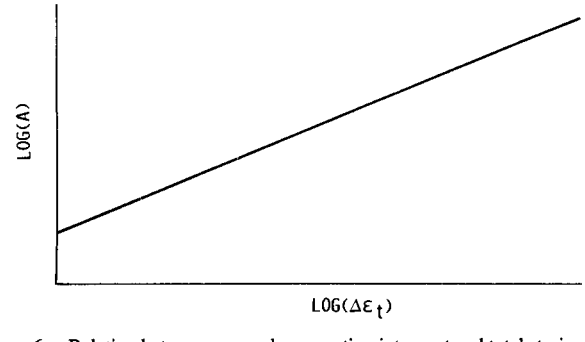

Figure 6.—Relation between power law equation intercept and total strainrange.

$$A = A'(\Delta\epsilon_t)^\alpha \tag{14}$$

thus

$$y = A'(\Delta\epsilon)^\alpha(t)^m \tag{15}$$

The dependent variable y is now a function of two independent variables, $\Delta\epsilon_t$ and t. If both sides of equation (15) are divided by $(\Delta\epsilon_t)^\alpha$, the family of lines shown schematically in figure 5 collapse to the single line of figure 7. The values of A', α, and m vary with the dependent variable y and the mechanical properties of the alloy. Note that TS-SRP is not dependent on the form of the equation used to correlate the flow data and that equation (15) could be of many different forms. The only requirement is that it represent the flow data in a tractable form with sufficient accuracy.

Five flow correlations based on equation (15) are used herein to determine the required flow variables: K_{ij}, F_{ij}, $\Delta\sigma$, σ_t, and σ_c. The first two are used to determine the coefficients B and C' in equation (9). The remaining three are used to determine the term R_σ in the mean stress correction using equation (12).

Note that, in principle, each of these correlations could be obtained directly from a suitable constitutive model. Although the exact form of the relations would no doubt differ somewhat from the one used here, the trends would be quite similar. The empirical correlations are used only because of their extreme simplicity and comparatively good accuracy.

For a specific alloy, these correlations depend on the maximum and minimum temperature of the cycle, the waveshape, how creep is introduced into the cycle (stress hold, strain hold, etc.), the straining rate during loading and unloading, and the phase relation between strain and temperature. Only inphase and out-of-phase continuous cycles and strain-hold cycles with zero mean strain are considered at the moment. These are shown in figure 4. When computing the stresses and strains for the postulated bithermal hysteresis loops, the temperature is changed at zero stress on the tension-going and compression-going sides of the loops. And when calculating the TMF loops, the temperature ramp rate is determined by the maximum and minimum temperatures in the cycle and the mechanical straining rate. The relation between strainrate and temperature rate for a sawtooth

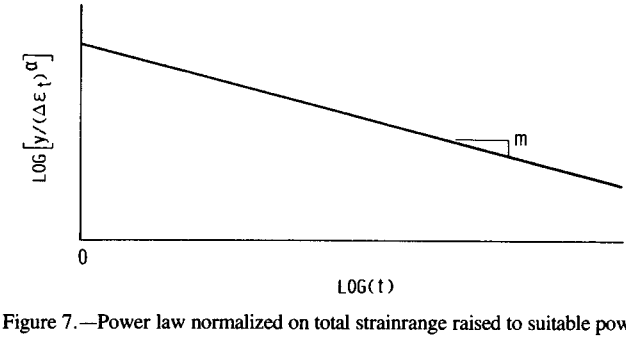

Figure 7.—Power law normalized on total strainrange raised to suitable power, collapsing family of lines shown in figure 5.

waveform is derived in the following manner for inphase and out-of-phase cycles. For a constant strainrate,

$$\dot{\epsilon} = 2f(\Delta\epsilon_t) \tag{16}$$

The period of one cycle is the reciprocal of the frequency f ($\tau = 1/f$), and the temperature range is traversed in one-half the cycle period.

Let τ' equal $\tau/2$, thus the time required to go from one strain limit to the other is

$$\tau' = \frac{\Delta\epsilon_t}{\dot{\epsilon}} \tag{17}$$

Let ΔT equal the temperature range of the cycle of interest (inphase or out-of-phase). The temperature ramp rate $\dot{T}$ is given by the temperature range divided by the time required to traverse the cycle. Note that $\dot{T}$ is positive if the temperature is increasing and negative if the temperature is decreasing;

$$\dot{T} = \frac{\Delta T(\Delta\epsilon_t)}{\dot{\epsilon}} \tag{18}$$

The inphase and out-of-phase thermomechanical and bithermal hysteresis loop results obtained from the Robinson model are given in table I and II, respectively, for the following conditions:

Total strainrange values
Continuous cycling: 0.002 to 0.010 in increments of 0.001
Strain-hold cycling: 0.002, 0.003, 0.004, 0.006, 0.008, 0.010
Hold time, sec: 60, 300, 600, 1800, 3600
Minimum temperature, °C: 250
Maximum temperature, °C: 600
Strainrate, in./in./min: 0.04

A review of the results of these computations for the cycles considered herein reveals the following differences in the stress-strain response of the thermomechanical and bithermal cycles for a given total strainrange and hold time.

Inphase cycles	Out-of-phase cycles
$\lvert\sigma_{t,tm}\rvert > \lvert\sigma_{t,bi}\rvert$	$\lvert\sigma_{t,tm}\rvert < \lvert\sigma_{t,bi}\rvert$
$\lvert\sigma_{c,tm}\rvert < \lvert\sigma_{c,bi}\rvert$	$\lvert\sigma_{c,tm}\rvert > \lvert\sigma_{c,bi}\rvert$
$\lvert\Delta\sigma_{tm}\rvert < \lvert\Delta\sigma_{bi}\rvert$	$\lvert\Delta\sigma_{tm}\rvert < \lvert\Delta\sigma_{bi}\rvert$
$\lvert\Delta\epsilon_{el,tm}\rvert < \lvert\Delta\epsilon_{el,bi}\rvert$	$\lvert\Delta\epsilon_{el,tm}\rvert < \lvert\Delta\epsilon_{el,bi}\rvert$

The above results are as expected. For example, in an inphase bithermal cycle, the stress is acting at the maximum temperature for the entire duration of the tensile half, but in a thermomechanical cycle the stress is acting at the maximum temperature only briefly at the maximum strain limit. Thus σ_t will be greater in a thermomechanical cycle than in a bithermal cycle because of the greater thermal recovery in the bithermal cycle. A similarly based argument also applies to σ_c.

We are now able to determine the flow correlations listed previously using equation (15), but first the strain-hardening exponent n in equation (6) must be determined using time-independent PP flow data. The strainrate of 0.04/min may not be fast enough to obtain time-independent (PP) deformation during loading and unloading but was the fastest rate used when the material constants for the model were determined. We have assumed that this rate produces no time-dependent inelastic strains. Note also that it is highly unlikely that the high-temperature ramp rate T implied by equation (18) could be achieved during the cooling leg of a thermomechanical cycle. Nevertheless, the following results were obtained:

$$\Delta\epsilon_{el} = 0.0045(\Delta\epsilon_{in})^{0.107} \tag{19}$$

for thermomechanical cycles and

$$\Delta\epsilon_{el} = 0.0044(\Delta\epsilon_{in})^{0.105} \tag{20}$$

for bithermal cycles. The relations for inphase and out-of-phase PP cycles are identical.

The differences between the thermomechanical and bithermal results are virtually nill under the current circumstances. These correlations are shown in figure 8 wherein the symbols represent values calculated using the Robinson model and the line represents the empirical correlation. Correlation coefficients of 0.990 and 0.995 for the thermomechanical and bithermal cycles, respectively, indicate an exceptionally good representation of the Robinson model. In the following, we present only results for TMF cycling.

Correlation Between Cyclic Strain-Hardening Coefficient and Hold Time

Equation (15) expressed for K_{ij} is as follows:

$$K_{ij} = A'(\Delta\epsilon_t)^{\alpha}(t)^m \tag{21}$$

The strain-hardening coefficient K_{ij} for each loading condition considered using the Robinson model (hold time, total strainrange, phase relation, etc.) is calculated using equation (6) and the proper value of the strain-hardening exponent from equations (19) and (20). Previously (ref. 3), K_{ij} was taken to be independent of total strainrange, but additional analysis indicates that it is a weak function of total strainrange. A multiple regression analysis of the appropriate values gives the following correlations for out-of-phase and inphase TMF cycling with $n = 0.107$:

$$\frac{K_{pc}}{(\Delta\epsilon_t)^{0.020}} = 4.689\times10^{-3}(t)^{-0.0167} \tag{22}$$

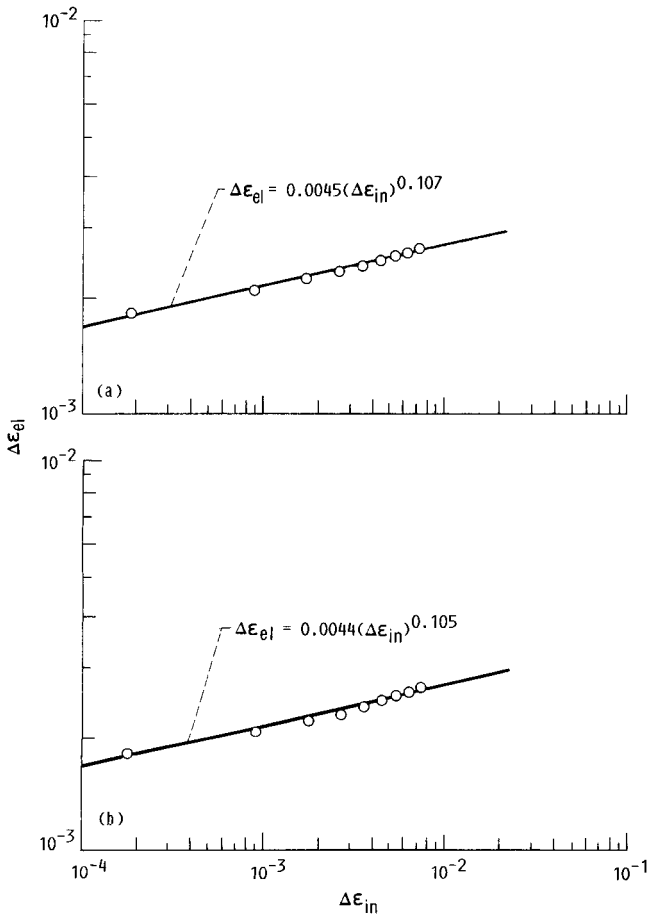

(a) Thermomechanical cycles; inphase and out-of-phase.
(b) Bithermal cycles; inphase and out-of-phase.

Figure 8.—Relation between elastic strainrange and inelastic strainrange for time-independent (PP) deformation for nonisothermal cycles. Alloy, 2-1/4Cr-1Mo steel in post-weld, heat-treated condition; minimum temperature, 250 °C, maximum temperature, 600 °C.

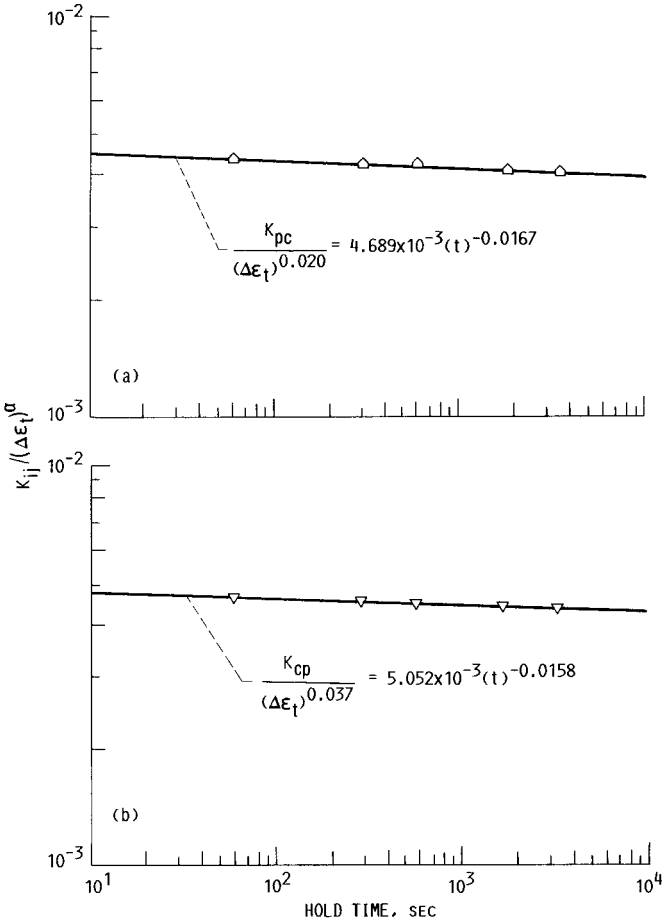

(a) PC cycles, out-of-phase.
(b) CP cycles, inphase.

Figure 9.—Relation between strain-hardening coefficient K_{ij} and hold time for thermomechanical strain-hold cycles. Alloy, 2-1/4Cr-1Mo steel in post-weld, heat-treated condition; minimum temperaure, 250 °C, maximum temperature, 600 °C; cyclic strain-hardening exponent, n, 0.107.

for out-of-phase cycling and

$$\frac{K_{cp}}{(\Delta\epsilon_t)^{0.037}} = 5.052\times10^{-3}(t)^{-0.0158} \qquad (23)$$

for inphase cycling. These equations are represented in figure 9, and their excellent ability to correlate the calculated results is shown in figure 10.

Correlation Between Strain Fraction and Hold Time

Equation (15) expressed for F_{ij} is as follows:

$$F_{ij} = A'(\Delta\epsilon_t)^{\alpha}(t)^{m} \qquad F_{ij} \leq 1.0 \qquad (24)$$

Analysis of the strain fraction—hold time data showed that equation (24) is not applicable over the entire range of the data. However, good correlations were obtained by dividing the data into two regimes as indicated below.
For $0.002 \leq \Delta\epsilon_t \leq 0.004$,

$$\frac{F_{pc}}{(\Delta\epsilon_t)^{-2.073}} = 1.416\times10^{-6}(t)^{0.0506} \qquad (25)$$

for out-of-phase cycles and

$$\frac{F_{cp}}{(\Delta\epsilon_t)^{-2.110}} = 1.204\times10^{-6}(t)^{0.0448} \qquad (26)$$

for inphase cycles. These equations are expressed in figure 11, and their ability to correlate the calculated results is represented by correlation coefficients of 0.993 and 0.994, respectively.

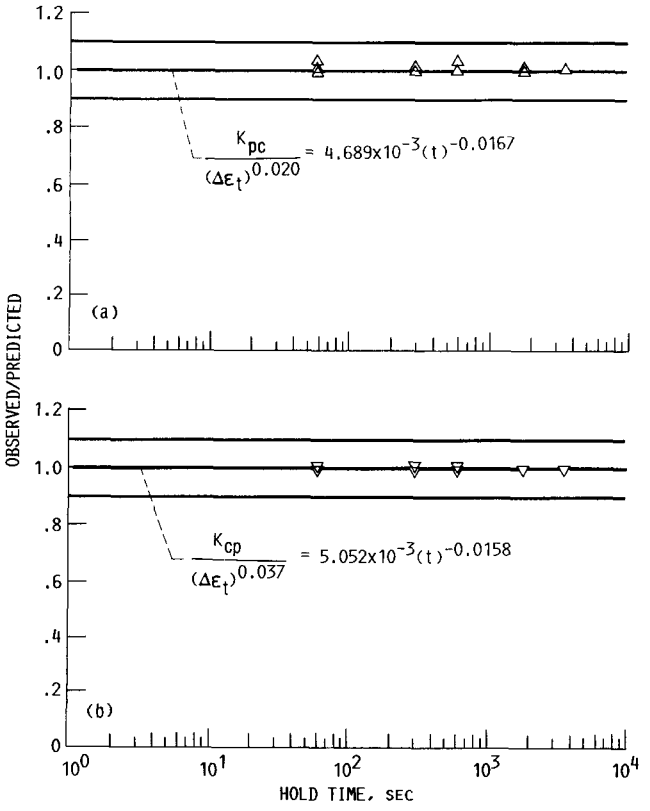

(a) PC cycles, out-of-phase.
(b) CP cycles, inphase.

Figure 10.—Ability of equation (21) to correlate cyclic strain-hardening coefficient K_{ij} with hold time for thermomechanical cycles. Alloy, 2-1/4Cr-1Mo steel in post-weld, heat-treated condition; minimum temperature 250 °C; maximum temperature, 600 °C.

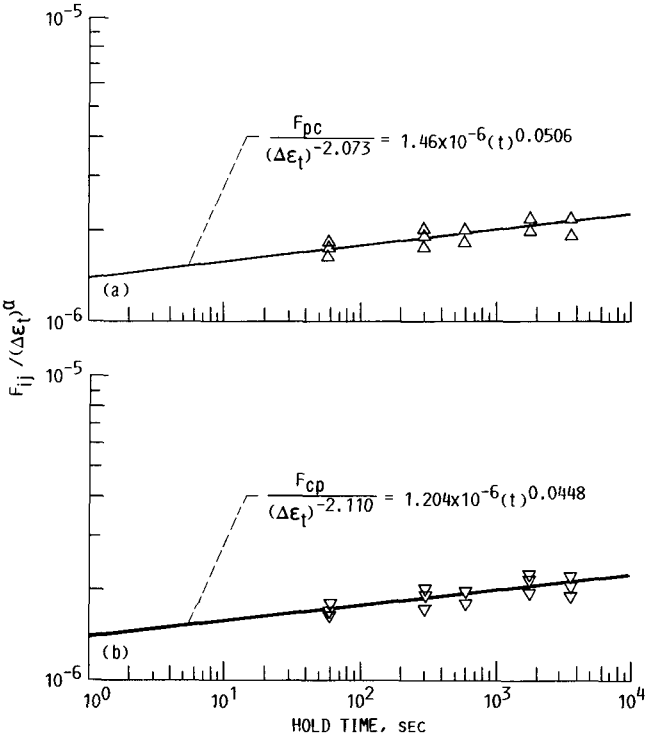

(a) PC cycles, out-of-phase.
(b) CP cycles, inphase.

Figure 11.—Relation between strain fraction F_{ij} and hold time for thermomechanical strain-hold cycles. Alloy, 2-1/4Cr-1Mo steel in post-weld, heat-treated condition; minimum temperature, 250 °C, maximum temperature, 600 °C; $0.002 \leq \Delta\epsilon_t \leq 0.004$.

For $0.004 \leq \Delta\epsilon_t \leq 0.010$,

$$\frac{F_{pc}}{(\Delta\epsilon_t)^{-1.367}} = 6.062\times10^{-5}(t)^{0.0744} \tag{27}$$

for out-of-phase cycles and

$$\frac{F_{cp}}{(\Delta\epsilon_t)^{-1.364}} = 6.166\times10^{-5}(t)^{0.0733} \tag{28}$$

for inphase cycles. These equations are expressed in figure 12, and the correlation coefficients are 0.999 and 0.997, respectively. The constants for the correlations for K_{ij} and F_{ij} for TMF cycling (eqs. (21) to (28)) are summarized in table III.

Correlations Between Stress and Hold Time

Our experience suggests that better correlations for σ_t and σ_c are usually obtained when σ_t is used for cycles where creep occurs in the tensile half of the hysteresis loop (CP cycle) and when σ_c is used where creep occurs on the compressive side of the loop (PC cycle). The results obtained here show that stress is a very weak function of hold time and could be omitted with little loss of accuracy. But this may not be true generally, and we have chosen to include it for illustrative purposes. The resulting stress correlations are summarized in table IV.

Life Prediction of TMF

In this section we outline the steps required to predict the life of a TMF cycle. For purposes of illustration, an inphase tensile strain-hold cycle (THIP) is selected. The mechanical strainrate and temperature limits are given in the previous section.

TMF cycles invariably contain both time-dependent and time-independent components of inelastic strain. Thus a THIP cycle will contain both PP and CP strain components, and the appropriate generic SRP inelastic strainrange versus life relations, equation (4), are required. Both relations must be for inphase cycling. Unfortunately, the numerical values of the material constants C_{ij} and c are not available at present.

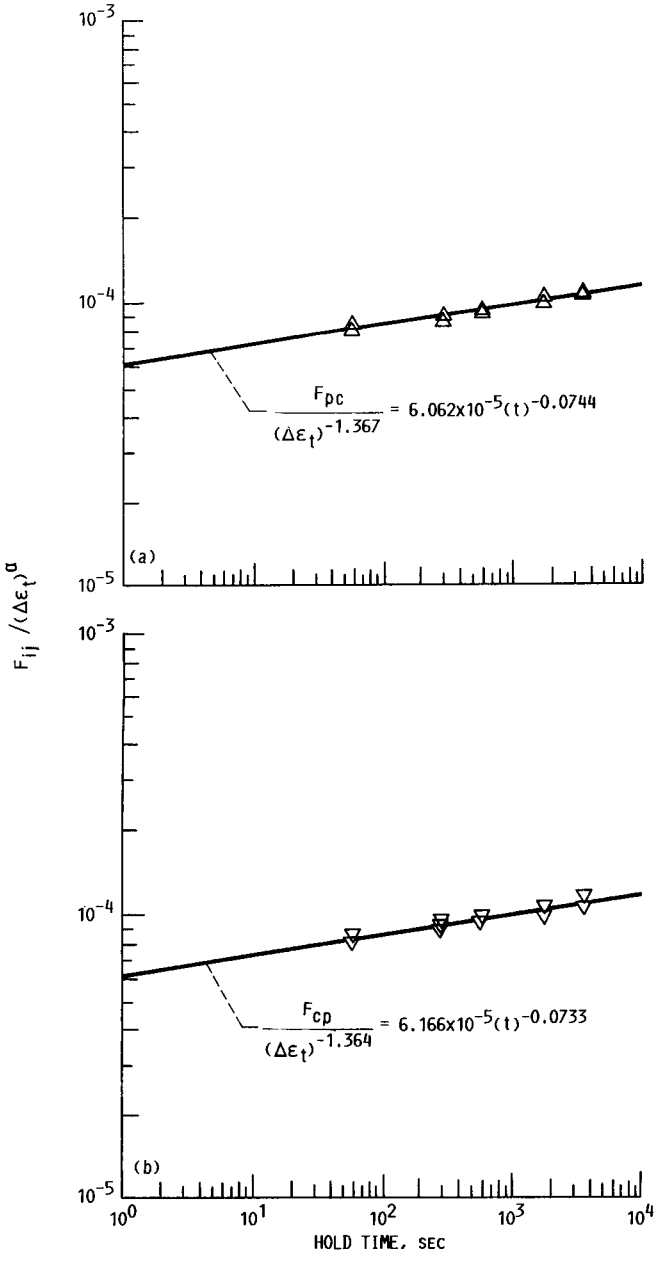

(a) PC cycles, out-of-phase.
(b) CP cycles, inphase.

Figure 12.—Relation between strain fraction F_{ij} and hold time for thermomechanical cycles. Alloy, 2-1/4Cr-1Mo steel in post-weld, heat-treated condition; minimum temperature, 250 °C; maximum temperature, 600 °C; $0.004 \leq \Delta\epsilon_t \leq 0.010$.

As discussed earlier, bithermal testing is recommended for determination of these material constants. For now, we proceed as if C_{ij} and c values are known;

$$\Delta\epsilon_{in} = C_{pp}(N_{pp})^c \tag{29}$$

$$\Delta\epsilon_{in} = C_{cp}(N_{cp})^c \tag{30}$$

The intercept C' of the equivalent inelastic line in equation (9) can now be determined. From equation (3),

$$C' = \left[F_{pp}(C_{pp})^{1/c} + F_{cp}(C_{cp})^{1/c}\right]^c \tag{31}$$

Since $F_{pp} = 1.0 - F_{cp}$, equation (3) can be rewritten as follows:

$$C' = \left[(C_{pp})^{1/c} - F_{cp}\left[(C_{pp})^{1/c} - (C_{cp})^{1/c}\right]\right]^c \tag{32}$$

The strain fraction F_{cp} is determined using the appropriate correlation given in the previous section.

If F_{cp} is very small ($\simeq 0$), $C' \simeq C_{pp}$; and if F_{cp} approaches unity, $C' \simeq C_{cp}$. The equivalent elastic line intercept B in equation (9) can now be determined using equation (7). The value of K_{cp} is determined using the correlation given in the previous section, and the value of C' is determined using equation (32);

$$B = K_{cp}(C')^n \tag{33}$$

The ingredients required to make a life prediction are now available. With a knowledge of $\Delta\epsilon_t$ and the proper constants for equation (9), we can now solve for N_{fo}. The value of N_{fo} can be determined by trial-and-error or by direct use of the inversion method given in reference 14. Note that N_{fo} is the cyclic life for a theoretical zero mean stress condition (ref. 10).

The final step in a life prediction is to account for the effects of mean stress on cyclic life. Rewriting equation (10) yields

$$N_{fm} = \left[(N_{fo})^b - V_{eff}\right]^{1/b} \tag{34}$$

The value of V_{eff} can be determined using equation (12) or some other method. If equation (12) is used, the values of σ_{min} and σ_{max} are obtained using the appropriate stress versus hold time correlations given by the constants in table IV.

Concluding Remarks

The total strainrange version of Strainrange Partitioning (TS–SRP) was developed originally for isothermal fatigue. This development makes it easier to characterize an alloy and predict cyclic life in the low-strain regime without having to conduct failure tests in this regime. This development is based on a derived relation between failure behavior and the cyclic stress-strain or flow response of an alloy. Failure testing is done only in the high-strain regime where test times and costs are more reasonable, and flow testing is done in both the high- and low-strain regime. The flow tests need be run only until the stress-strain hysteresis loop approaches cyclic stability. Failure tests should also be done to determine the effects of mean stress on cyclic life. If mean stress effects are not

accounted for, inaccurate life predictions will result from using this or any other life-prediction method in the low-strain, long-life regime.

A method for extending TS-SRP to characterize an alloy and predict the lives of thermomechanical cycles in the low-strain regime is presented. This method is based on nonisothermal rather than isothermal data. Bithermal fatigue testing is recommended at this time to generate the nonisothermal data required to determine the inelastic strainrange-life relations required by TS-SRP. Bithermal fatigue testing offers the simplicity of isothermal testing but captures the first-order effects of inphase and out-of-phase TMF cycling. Thermomechanical flow tests would normally be conducted to properly characterize the stress-strain response, but bithermal flow tests could be conducted at the lower strainranges where the inelastic strains are small, and it is difficult to analyze the thermomechanical hysteresis loops.

The data from flow testing are used to determine flow response of an alloy. This response is approximated using a simple power law with two independent variables with constants determined by a multiple regression analysis. These same power law relations were used in the isothermal version of TS-SRP. It is not a requirement that this particular power law be used, since any relation could be used provided it accurately represents the data. Currently, there are no TMF data to validate the proposed life-prediction method.

Lewis Research Center
National Aeronautics and Space Administration
Cleveland, Ohio, November 4, 1987

Appendix—Analysis for Nonparallel Failure Lines

Our experience strongly suggests that the assumption that inelastic and elastic strainrange versus life lines for creep-fatigue cycles are parallel to the corresponding lines for pure fatigue or PP cycles is reasonable for isothermal creep-fatigue analysis. On this basis, we have extended this assumption to nonisothermal creep-fatigue. However, this assumption may not be applicable for all alloys, and a method would be required for dealing with such a problem.

If the assumption of parallel lines is not reasonable, then the equations relating failure and flow behavior given here are not applicable. For purposes of discussion, let us assume that the inelastic failure lines for creep-fatigue cycles (PC, CP, CC) cycles are not parallel to the PP line or to each other and that the elastic failure lines for these cycles both translate and rotate as a function of hold time.

Failure behavior is now expressed by the following equations:

$$\Delta\epsilon_{el} = B(N_{fo})^{b'} \tag{35}$$

where

$$b' = b'(t)$$

The four generic SRP life relations are

$$\Delta\epsilon_{in} = C_{pp}(N_{pp})^{c} \tag{36}$$

for PP cycles and

$$\Delta\epsilon_{in} = C_{ij}(N_{ij})^{c^*} \tag{37}$$

for PC, CP, and CC cycles, where c^* is not equal to c and c^* may be different for each type of cycle.

The interaction damage rule (IDR) is written as follows for a creep-fatigue cycle:

$$\frac{F_{pp}}{N_{pp}} + \frac{F_{ij}}{N_{ij}} = \frac{1}{N_{fo}} \tag{38}$$

Using equations (36) and (37), we obtain the following:

$$F_{pp}\left(\frac{C_{pp}}{\Delta\epsilon_{in}}\right)^{1/c} + F_{ij}\left(\frac{C_{ij}}{\Delta\epsilon_{in}}\right)^{1/c^*} = \frac{1}{N_{fo}} \tag{39}$$

and solving for $\Delta\epsilon_{in}$ we obtain

$$\Delta\epsilon_{in} = C''(N_{fo})^{c} \tag{40}$$

where

$$C'' = [F_{pp}(C_{pp})^{1/c} + F_{ij}(C_{ij})^{1/c^*}(\Delta\epsilon_{in})^{1/c-1/c^*} \tag{41}$$

Flow behavior is expressed by the following equation:

$$\Delta\epsilon_{el} = K_{ij}(\Delta\epsilon_{in})^{n'} \tag{43}$$

Setting equation (35) equal to equation (43) and eliminating N_{fo} using equation (40) we obtain

$$B = K_{ij}(C'')^{n'} \tag{44}$$

where $n' = b'/c$.

Since the total strain version of Strainrange Partitioning (TS-SRP) is intended for the low-strain regime where the elastic strainrange is the dominate term in equation (8), it is reasonable to retain the assumption of parallel inelastic lines and to allow the elastic line to both translate and rotate with hold time. Assuming the inelastic lines to be parallel simplifies the analysis considerably, but does not introduce large errors. Thus equation (9) becomes

$$\Delta\epsilon_t = B(N_{fo})^{b'} + C'(N_{fo})^{c} \tag{45}$$

where $b' = b'(t)$. Since b' is time dependent, it then follows that the strain-hardening exponent n' in equation (43) is also time dependent. The $\Delta\epsilon_{el} - \Delta\epsilon_{in}$ line both translates and rotates with time. Thus, equation (15) cannot be used to determine K_{ij} since this equation accounts only for translation.

The time dependency of the fatigue exponent b' in equation (45) can be determined by conducting flow tests to characterize the time dependency of the strain-hardening exponent n' in equation (43). At this time we are unable to suggest a suitable form for the equations for K_{ij} and n', but we feel that equation (15) can still be used to correlate the strain fractions F_{ij} and the stress terms $\Delta\sigma$, σ_t, and σ_c.

When the life relations are nonparallel, failure testing will have to include tests at lower strainranges to characterize this more complex material behavior.

References

1. Manson, S.S.; Halford, G.R.; and Hirschberg, M.H.: Creep-Fatigue Analysis by Strain-Range Partitioning. Design for Elevated Temperature Environment, S.Y. Zamrik, ed., ASME, 1971, pp. 12-28. (NASA TM X-67838.)
2. Halford, G.R.; and Saltsman, J.F.: Strainrange Partitioning—A Total Strain Range Version. ASME International Conference on Advances in Life Prediction Methods, D.A. Woodford and J.R. Whitehead, eds., ASME, 1983, pp. 17-26.
3. Saltsman, J.F.; and Halford, G.R.: An Update of the Total Strain Version of SRP. Symposium on Low Cycle Fatigue—Directions for the Future, ASTM, STP-942, ASTM, 1987.
4. Halford, G.R., et al.: Bithermal Fatigue, a Link Between Isothermal and Thermomechanical Fatigue. Symposium on Low Cycle Fatigue—Directions for the Future, ASTM STP-942, ASTM, 1987, pp. 625-637.
5. Halford, G.R.; and Manson, S.S.: Life Prediction of Thermal-Mechanical Fatigue Using Strainrange Partitioning. Thermal Fatigue of Materials and Components, ASTM STP-612, D.A. Spera and D.F. Mowbray, eds., ASTM, 1976, pp.239-254. (NASA TM X-71829.)
6. Robinson, D.N.; and Swinderman, R.W.: Unified Creep-Plasticity Constitutive Equations for 2-1/4Cr-1Mo Steel at Elevated Temperature. ORNL/TM-8444, 1982.
7. Coffin, L.F., Jr.,: The Effect of Frequency on High Temperature Low Cycle Fatigue. Proceedings of the Air Force Conference on Fatigue and Fracture of Aircraft Structures and Materials, AFFDL-TR-70-144, 1970, pp. 301-312.
8. Manson, S.S.: The Challenge to Unify Treatment of High Temperature Fatigue—A Partisan Proposal Based on Strainrange Partitioning. Fatigue at Elevated Temperatures, ASTM STP-520, A.E. Carden, A.J. McEvily, and C.H. Wells, eds., ASTM, 1973, pp. 744-775. (NASA TM X-68171.)
9. Kalluri, S.; Manson, S.S.; and Halford, G.R.: Environmental Degradation of 316 Stainless Steel in High Temperature Fatigue, Proceedings, Third International Conference on Environmental Degradation of Engineering Materials, Penn State Univ., 1987, pp. 503-519. (NASA TM-89931.)
10. Halford, G.R.; and Nachtigall, A.J.: Strainrange Partitioning Behavior of an Advanced Gas Turbine Alloy, AFE-1DA. J. Aircr., vol. 17, no. 8, Aug. 1980, pp. 598-604.
11. Halford, G.R.: Low-Cycle Thermal Fatigue. Thermal Stresses II, R.B. Hetnarski, ed., Elsevier, 1987, pp. 329-428.
12. Halford, G.R.; Saltsman, J.F.; and Hirschberg, M.H.: Ductility-Normalized Strainrange Partitioning Life Relations for Creep-Fatigue Life Prediction. Environmental Degradation of Engineering Materials, M.R. Louthan and R.P. McNitt, eds., Virginia Polytechnic Institute and State Univ., Blacksburg, VA, 1977, pp. 599-612.
13. Chang, T.Y.; and Thompson, R.L.: A Computer Program for Predicting Nonlinear Uniaxial Material Responses Using Viscoplastic Models. NASA TM-83675, 1984.
14. Manson, S.S.; and Muralidharan, U.: A Single Expression Formula for Inverting Strain-Life and Stress-Strain Relationships. NASA CR-165347, 1981.

TABLE I.—RESULTS OF FLOW CALCULATIONS FOR THERMOMECHANICAL CYCLES USING THE ROBINSON MODEL

[Alloy, 2-1/4Cr-1Mo steel in post-weld, heat-treated condition.]

Specimen number	Test type	Temperature, °C		Rate data				Stresses, MPa					
				Strainrate, percent/sec		Hold time, sec		Ten.[a] max.	Comp.[b] max.	Range max.	Relaxation		Mean / amp.[c]
		Ten.[a]	Comp.[b]	Ten.[a]	Comp.[b]	Ten.[a]	Comp.[b]				Ten.[a]	Comp.[b]	
1	HRIP	600	250	6.7E-02	6.7E-02	0	0	102.0	217.7	319.7	0.0	0.0	-0.362
2								121.6	253.7	375.3			-0.352
3								132.5	269.3	401.8			-0.340
4								140.4	280.1	420.5			-0.332
5								147.1	288.3	435.4			-0.324
6								152.5	295.7	448.2			-0.320
7								157.8	301.3	459.1			-0.313
8								161.8	307.2	469.0			-0.310
9								166.4	311.8	478.2			-0.304
10	HROP	250	600					217.2	102.7	319.9			0.358
11								253.2	122.5	375.7			0.348
12								268.7	133.4	402.1			0.336
13								279.3	141.3	420.6			0.328
14								287.5	148.2	435.6			0.320
15								294.8	153.4	448.2			0.315
16								300.4	159.1	459.5			0.308
17								306.3	163.0	469.3			0.305
18								310.8	167.6	478.4			0.299
19	THIP	600	250			60.0		98.2	231.7	329.9	39.2		-0.405
20						300.0		97.6	233.7	331.2	46.3		-0.411
21						600.0		97.7	234.4	331.2	49.1		-0.413
22						1800.0		97.0	235.3	332.3	52.9		-0.416
23						3600.0		96.8	235.8	332.6	55.1		-0.418
24						60.0		121.2	258.0	379.2	46.3		-0.361
25						300.0		121.1	258.6	379.8	53.0		-0.362
26						600.0		121.1	258.9	380.1	55.7		-0.363
27						1800.0		121.1	259.2	380.3	59.5		-0.363
28						3600.0		121.1	259.4	380.5	61.5		-0.363
29						60.0		132.4	272.0	404.4	47.4		-0.345
30						300.0		132.4	272.4	404.8	54.1		-0.346
31						600.0		132.4	272.6	404.9	56.6		-0.346
32						1800.0		132.3	272.8	405.1	60.3		-0.347
33						3600.0		132.3	273.0	405.3	62.5		-0.347
34						60.0		147.0	290.1	437.1	48.0		-0.327
35						300.0		147.0	290.5	437.3	54.8		-0.328
36						600.0		147.0	290.5	437.5	57.4		-0.328
37						1800.0		147.0	290.7	437.7	61.6		-0.328
38						3600.0		147.0	290.8	437.8	64.5		-0.328
39	THIP	600	250	6.7E-02	6.7E-02	60.0	0	158.2	302.8	460.9	48.3	0.0	-0.314

[a]Tension.
[b]Compression.
[c]Amplitude.

TABLE I.—Continued.

Specimen number	Strainrange values, percent						
	Total	Elastic	Inelastic	PP	PC	CP	CC
1	0.200	0.181	0.019	0.019	0.000	0.000	0.000
2	.300	.209	.091	.091			
3	.400	.224	.176	.176			
4	.500	.234	.266	.266			
5	.600	.242	.358	.358			
6	.700	.249	.451	.451			
7	.800	.256	.544	.544			
8	.900	.262	.638	.638			
9	1.000	.269	.731	.731			
10	.200	.182	.018	.018			
11	.300	.209	.091	.091			
12	.400	.224	.176	.176			
13	.500	.234	.266	.266			
14	.600	.243	.357	.357			
15	.700	.249	.451	.451			
16	.800	.256	.544	.544			
17	.900	.262	.638	.638			
18	1.000	.269	.731	.731			
19	.200	.164	.036	.009		.027	
20		.161	.039	.007		.032	
21		.158	.042	.008		.034	
22		.156	.044	.007		.037	
23		.155	.045	.007		.038	
24	.300	.184	.116	.083		.033	
25		.180	.120	.083		.037	
26		.179	.121	.082		.039	
27		.176	.124	.082		.042	
28		.175	.125	.082		.043	
29	.400	.197	.203	.170		.033	
30		.193	.207	.169		.038	
31		.191	.209	.170		.039	
32		.189	.211	.168		.043	
33		.188	.212	.168		.044	
34	.600	.214	.386	.352		.034	
35		.210	.390	.351		.039	
36		.208	.392	.352		.040	
37		.205	.395	.352		.043	
38		.204	.396	.350		.046	
39	.800	.227	.573	.539	0.000	.034	0.000

TABLE I.—Continued.

Specimen number	Test type	Temperature, °C		Rate data				Stresses, MPa					
				Strainrate, percent/sec		Hold time, sec		Ten.[a] max.	Comp.[b] max.	Range max.	Relaxation		Mean amp.[c]
		Ten.[a]	Comp.[b]	Ten.[a]	Comp.[b]	Ten.[a]	Comp.[b]				Ten.[a]	Comp.[b]	
40	THIP	600	250	6.7E-02	6.7E-02	300.0	0	158.2	303.0	461.1	55.3	0.0	-0.314
41						600.0		158.2	303.1	461.3	58.3		-0.314
42						1800.0		158.2	303.3	461.5	63.4		-0.314
43						3600.0		158.1	303.4	461.5	67.6		-0.315
44						60.0		166.3	313.1	479.4	48.1		-0.306
45						300.0			313.6	479.9	55.6		-0.307
46						600.0			313.4	479.8	58.9		-0.307
47						1800.0			313.7	480.0	65.5		-0.307
48						3600.0			313.8	480.1	71.3		-0.307
49	CHOP	250	600			0	60.0	229.3	99.6	328.9	0.0	33.4	0.394
50							300.0	232.6	98.5	331.0		43.8	0.405
51							600.0	230.7	99.4	330.1		38.2	0.398
52							1800.0	234.9	97.6	332.5		53.0	0.413
53							3600.0	234.8	97.6	332.5		53.0	0.413
54							60.0	257.5	122.1	379.6		46.0	0.357
55							300.0	257.7	122.0	379.8		49.2	0.357
56							600.0	258.9		380.9		61.5	0.359
57							1800.0	258.6		380.6		59.1	0.359
58							3600.0	258.4		380.3		56.0	0.359
59							60.0	271.3	133.2	404.5		47.3	0.341
60							300.0	271.7		404.9		53.2	0.342
61							600.0	271.7		404.9		53.6	0.342
62							1800.0	272.2		405.4		61.6	0.343
63							3600.0	272.3		405.5		62.3	0.343
64							60.0	289.3	148.0	437.2		48.0	0.323
65							300.0	289.6		437.6		54.5	0.324
66							600.0	289.7		437.7		56.8	0.324
67							3600.0	290.1		438.1		65.4	0.324
68							60.0	301.9	158.9	460.8		48.3	0.310
69							300.0	302.1	158.9	461.0		55.2	0.311
70							600.0	302.2	159.0	464.2		58.0	0.308
71							1800.0	302.5	159.1	461.6		62.5	0.311
72							3600.0	302.6	159.1	461.8		69.4	0.311
73							60.0	312.1	167.5	479.7		48.2	0.301
74							300.0	312.2		479.8		55.6	0.302
75							600.0	312.3		479.9		58.9	0.302
76							1800.0	312.8		480.3		65.6	0.303
77	CHOP	250	600	6.7E-02	6.7E-02	0	3600.0	312.6	167.5	480.2	0.0	69.4	0.302

[a]Tension.
[b]Compression.
[c]Amplitude.

TABLE I.—Concluded.

Specimen number	Strainrange values, percent						
	Total	Elastic	Inelastic	PP	PC	CP	CC
40	0.800	0.221	0.579	0.541	0.000	0.038	0.000
41	↓	.220	.580	.539	↓	.041	↓
42	↓	.217	.583	.538	↓	.045	↓
43	↓	.214	.586	.539	↓	.047	↓
44	1.000	.239	.761	.728	↓	.033	↓
45	↓	.234	.766	.727	↓	.039	↓
46	↓	.232	.768	.726	↓	.042	↓
47	↓	.227	.773	.727	↓	.046	↓
48	↓	.223	.777	.727	↓	.050	↓
49	.200	.168	.032	.009	.023	0.000	↓
50	↓	.161	.039	.008	.031	↓	↓
51	↓	.164	.036	.010	.026	↓	↓
52	↓	.157	.043	.006	.037	↓	↓
53	↓	.157	.043	.006	.037	↓	↓
54	.300	.185	.115	.083	.032	↓	↓
55	↓	.183	.117	.082	.035	↓	↓
56	↓	.175	.125	.082	.043	↓	↓
57	↓	.176	.124	.082	.042	↓	↓
58	↓	.178	.122	.082	.040	↓	↓
59	.400	.198	.202	.169	.033	↓	↓
60	↓	.193	.207	.170	.037	↓	↓
61	↓	.194	.206	.168	.038	↓	↓
62	↓	.191	.209	.166	.043	↓	↓
63	↓	.188	.212	.168	.044	↓	↓
64	.600	.215	.385	.351	.034	↓	↓
65	↓	.210	.390	.352	.038	↓	↓
66	↓	.208	.392	.352	.040	↓	↓
67	↓	.203	.397	.351	.046	↓	↓
68	.800	.227	.573	.539	.034	↓	↓
69	↓	.222	.578	.539	.039	↓	↓
70	↓	.221	.579	.538	.041	↓	↓
71	↓	.218	.582	.538	.044	↓	↓
72	↓	.213	.587	.538	.049	↓	↓
73	1.000	.239	.761	.727	.034	↓	↓
74	↓	.234	.766	.727	.039	↓	↓
75	↓	.227	.773	.732	.041	↓	↓
76	↓	.227	.773	.727	.046	↓	↓
77	1.000	.224	.776	.728	.048	0.000	0.000
****	FLOW TEST						

TABLE II.—RESULTS OF FLOW CALCULATIONS FOR BITHERMAL CYCLES USING THE ROBINSON MODEL

[Alloy, 2-1/4Cr-1Mo steel in post-weld, heat-treated condition.]

Specimen number	Test type	Temperature, °C		Rate data				Stresses, MPa					
				Strainrate, percent/sec		Hold time, sec		Ten.[a] max.	Comp.[b] max.	Range max.	Relaxation		Mean amp.[c]
		Ten.[a]	Comp.[b]	Ten.[a]	Comp.[b]	Ten.[a]	Comp.[b]				Ten.[a]	Comp.[b]	
1	HRIP	600	250	6.7E-02	6.7E-02	0	0	98.4	235.3	333.7	0.0	0.0	-0.410
2								117.8	268.3	386.1			-0.390
3								130.7	280.5	411.2			-0.364
4								139.1	289.2	428.3			-0.350
5								145.9	296.2	442.1			-0.340
6								151.8	302.3	454.1			-0.331
7								157.1	307.7	464.8			-0.324
8								160.4	312.5	472.9			-0.322
9								166.1	316.9	483.0			-0.312
10	HROP	250	600					230.7	99.0	329.7			0.399
11								267.4	118.5	385.9			0.386
12								279.6	129.8	409.4			0.366
13								288.3	138.2	426.6			0.352
14								295.3	145.1	440.5			0.341
15								301.4	151.2	452.6			0.332
16								306.6	156.3	462.9			0.325
17								311.9	160.4	472.3			0.321
18								316.0	165.5	481.5			0.313
19	THIP	600	250			60.0		94.8	251.5	346.3	36.2		-0.452
20						300.0		94.2	253.8	348.0	43.1		-0.459
21						600.0		94.0	254.6	348.6	45.9		-0.461
22						1800.0		93.7	255.7	349.4	49.8		-0.464
23						3600.0		93.6	256.4	349.9	52.0		-0.465
24						60.0		117.4	272.4	389.8	117.4		-0.398
25						300.0			273.1	390.5	50.4		-0.399
26						600.0			273.4	390.7	53.0		-0.399
27						1800.0			273.7	391.1	56.8		-0.400
28						3600.0			273.9	391.3	58.9		-0.400
29						60.0		128.9	283.5	412.3	45.2		-0.375
30						300.0		128.8	283.7	412.5	51.9		-0.376
31						600.0			283.9	412.7	54.4		-0.376
32						1800.0			284.1	412.9	58.1		-0.376
33						3600.0			284.3	413.1	60.3		-0.376
34						60.0		144.0	298.2	442.2	46.3		-0.349
35						300.0			298.5	442.5	53.1		-0.349
36						600.0			298.6	442.7	55.7		-0.349
37						1800.0			298.8	442.8	59.8		-0.350
38						3600.0			298.9	442.9	62.5		-0.350
39	THIP	600	250	6.7E-02	6.7E-02	60.0	0	155.2	309.2	464.4	47.0	0.0	-0.332

[a]Tension.
[b]Compression.
[c]Amplitude.

TABLE II.—Continued.

Specimen number	Strainrange values, percent						
	Total	Elastic	Inelastic	PP	PC	CP	CC
1	0.200	0.182	0.018	0.018	0.000	0.000	0.000
2	.300	.209	.091	.091			
3	.400	.223	.177	.177			
4	.500	.233	.267	.267			
5	.600	.242	.358	.358			
6	.700	.250	.450	.450			
7	.800	.257	.543	.543			
8	.900	.263	.637	.637			
9	1.000	.269	.731	.731			
10	.200	.181	.019	.019			
11	.300	.208	.092	.092			
12	.400	.222	.178	.178			
13	.500	.233	.267	.267			
14	.600	.241	.359	.359			
15	.700	.250	.450	.450			
16	.800	.256	.544	.544			
17	.900	.263	.637	.637			
18	1.000	.269	.731	.731			
19	.200	.163	.037	.011		.026	
20		.159	.041	.011		.030	
21		.158	.042	.010		.032	
22		.155	.045	.010		.035	
23		.153	.047	.010		.037	
24	.300	.184	.116	.086		.030	
25		.179	.121			.035	
26		.177	.123			.037	
27		.175	.125			.039	
28		.173	.127			.041	
29	.400	.196	.204	.173		.031	
30		.191	.209	.173		.036	
31		.189	.211	.173		.038	
32		.188	.212	.172		.040	
33		.186	.214	.172		.042	
34	.600	.214	.386	.354		.032	
35		.209	.391			.037	
36		.207	.393			.039	
37		.204	.396			.042	
38		.202	.398			.044	
39	.800	.227	.573	.540	0.000	.033	0.000

TABLE II.—Continued.

Specimen number	Test type	Temperature, °C		Rate data				Stresses, MPa					
				Strainrate, percent/sec		Hold time, sec		Ten.[a] max.	Comp.[b] max.	Range max.	Relaxation		Mean / amp.[c]
		Ten.[a]	Comp.[b]	Ten.[a]	Comp.[b]	Ten.[a]	Comp.[b]				Ten.[a]	Comp.[b]	
40	THIP	600	250	6.7E-02	6.7E-02	300.0	0	155.2	309.5	464.7	53.9	0.0	-0.332
41						600.0			309.6	464.8	56.7		-0.332
42						1800.0			309.8	465.0	61.7		-0.332
43						3600.0			309.9	465.1	65.7		-0.333
44						60.0		164.3	318.3	482.6	47.4		-0.319
45						300.0			318.6	482.9	54.7		-0.320
46						600.0			318.7	483.0	57.9		-0.320
47						1800.0			318.9	483.2	64.3		-0.320
48						3600.0			319.1	483.4	69.8		-0.320
49	CHOP	250	600			0	60.0	249.5	95.4	344.9	0.0	32.6	0.447
50							300.0	252.2	94.6	346.7		40.1	0.455
51							600.0	251.8	94.5	346.3		38.4	0.454
52							3600.0	255.5	93.8	349.4		50.8	0.463
53							60.0	271.7	118.2	389.9		43.5	0.394
54							300.0	272.1	118.1	390.3		47.6	0.395
55							600.0	273.5	118.0	391.5		60.4	0.397
56							1800.0	273.0	118.0	391.1		56.8	0.396
57							3600.0	273.0	118.1	391.1		55.9	0.396
58							60.0	282.5	129.6	412.1		45.2	0.371
59							300.0	282.9		412.5		51.1	0.372
60							600.0	283.0		412.6		52.1	0.372
61							1800.0	283.5		413.1		59.8	0.373
62							3600.0	283.5		413.1		60.3	0.373
63							60.0	297.3	145.0	442.3		46.4	0.344
64							300.0	297.6		442.6		52.9	0.345
65							600.0	297.7		442.7		55.2	0.345
66							1800.0	297.5		442.5		52.5	0.345
67							3600.0	298.1		443.1		63.7	0.346
68							60.0	308.2	156.2	464.4		47.0	0.327
69							300.0	308.4		464.7		53.8	0.328
70							600.0	308.6		464.8		56.5	
71							1800.0	308.7		464.9		60.9	
72							3600.0	309.0		465.2		68.2	
73							60.0	317.4	165.5	482.9		47.4	0.315
74							300.0	317.6		483.1		54.7	
75							600.0	317.4		482.9		57.9	
76							1800.0	317.9		483.4		64.3	
77	CHOP	250	600	6.7E-02	6.7E-02	0	3600.0	318.1	165.5	483.5	0.0	68.7	0.316

[a]Tension.
[b]Compression.
[c]Amplitude.

TABLE II.—Concluded.

Specimen number	Strainrange values, percent						
	Total	Elastic	Inelastic	PP	PC	CP	CC
40	0.800	0.222	0.578	0.540	0.000	0.038	0.000
41	↓	.220	.580	↓	↓	.040	↓
42	↓	.217	.583	↓	↓	.043	↓
43	↓	.214	.586	↓	↓	.046	↓
44	1.000	.238	.762	.729	↓	.033	↓
45	↓	.233	.767	↓	↓	.038	↓
46	↓	.231	.769	↓	↓	.040	↓
47	↓	.226	.774	↓	↓	.045	↓
48	↓	.222	.778	↓	↓	.049	↓
49	.200	.166	.034	.011	.023	0.000	↓
50	↓	.161	.039	.011	.028	↓	↓
51	↓	.161	.039	.012	.027	↓	↓
52	↓	.154	.046	.010	.036	↓	↓
53	.300	.183	.117	.086	.031	↓	↓
54	↓	.181	.119	.085	.034	↓	↓
55	↓	.172	.128	↓	.043	↓	↓
56	↓	.175	.125	↓	.040	↓	↓
57	↓	.176	.124	↓	.039	↓	↓
58	.400	.196	.204	.172	.032	↓	↓
59	↓	.192	.208	↓	.036	↓	↓
60	↓	.191	.209	↓	.037	↓	↓
61	↓	.186	.214	↓	.042	↓	↓
62	↓	.186	.214	↓	.042	↓	↓
63	.600	.213	.387	.354	.033	↓	↓
64	↓	.210	.390	.353	.037	↓	↓
65	↓	.208	.392	.353	.039	↓	↓
66	↓	.209	.391	.354	.037	↓	↓
67	↓	.202	.398	.353	.045	↓	↓
68	.800	.227	.573	.540	.033	↓	↓
69	↓	.222	.578	↓	.038	↓	↓
70	↓	.220	.580	↓	.040	↓	↓
71	↓	.217	.583	↓	.043	↓	↓
72	↓	.213	.587	.539	.048	↓	↓
73	1.000	.238	.762	.729	.033	↓	↓
74	↓	.233	.767	.729	.038	↓	↓
75	↓	.231	.769	.729	.040	↓	↓
76	↓	.227	.773	.728	.045	↓	↓
77	1.000	.224	.776	.728	.048	0.000	0.000
**** FLOW TEST							

TABLE III.—CONSTANTS FOR K_{ij} AND F_{ij} CORRELATIONS FOR THERMOMECHANICAL STRAIN-HOLD CYCLING FOR $y = A'(\Delta\epsilon_t)^{\alpha}(t)^{m}$

[Material, 2-1/4Cr-1Mo steel; post-weld, heat-treated condition.]

Cycle type	Total strain-range, $\Delta\epsilon_t$	Flow variable, y	Constant, A'	Power on total strain-range, α	Power of time, m	Correlation coefficient, r
PC (out-of-phase)	-------	K_{pc}	4.689×10^{-3}	0.020	−0.0167	0.857
	0.002 to 0.004	F_{pc}	1.416×10^{-6}	−2.073	.0506	.993
	0.004 to 0.010	F_{pc}	6.062×10^{-5}	−1.367	.0744	.999
CP (inphase)	-------	K_{cp}	5.052×10^{-3}	0.037	−0.0158	0.929
	0.002 to 0.004	F_{cp}	1.204×10^{-6}	−2.110	.0448	.994
	0.004 to 0.010	F_{cp}	6.166×10^{-5}	−1.364	.0733	.997

TABLE IV.—CONSTANTS[a] FOR STRESS CORRELATIONS FOR THERMOMECHANICAL STRAIN-HOLD CYCLING FOR $y = A'(\Delta\epsilon_t)^{\alpha}(t)^{m}$

[Material, 2-1/4Cr-1Mo steel; post-weld, heat-treated condition.]

Cycle type	Flow variable, y	Constant, A'	Power on total strain-range, α	Power of time, m	Correlation coefficient, r
PC	$\Delta\sigma$	1394.7	0.230	0.0008	0.990
	σ_c	722.3	.183	.0019	.989
CP	$\Delta\sigma$	1379.8	0.227	0.0008	0.987
	σ_t	781.4	.329	.0007	.986

[a]Stresses in units of MPa (1 ksi = 6.895 MPa).

NASA
National Aeronautics and Space Administration

Report Documentation Page

1. Report No.	2. Government Accession No.	3. Recipient's Catalog No.
NASA TP-2779		

4. Title and Subtitle
Life Prediction of Thermomechanical Fatigue Using Total Strain Version of Strainrange Partitioning (SRP)—A Proposal

5. Report Date
February 1988

6. Performing Organization Code

7. Author(s)
James F. Saltsman and Gary R. Halford

8. Performing Organization Report No.
E-3795

10. Work Unit No.
553-13-00

9. Performing Organization Name and Address
National Aeronautics and Space Administration
Lewis Research Center
Cleveland, Ohio 44135-3191

11. Contract or Grant No.

13. Type of Report and Period Covered
Technical Paper

12. Sponsoring Agency Name and Address
National Aeronautics and Space Administration
Washington, D.C. 20546-0001

14. Sponsoring Agency Code

15. Supplementary Notes
Substantial portions of this work appear in NASA CP-2493

16. Abstract

A method is proposed (without experimental verification) for extending the total strain version of Strainrange Partitioning (TS-SRP) to predict the lives of thermomechanical fatigue (TMF) cycles. The principal feature of TS-SRP is the determination of the time-temperature-waveshape dependent elastic strainrange versus life lines that are added subsequently to the classical inelastic strainrange versus life lines to form the total strainrange versus life relations. The procedure is based on a derived relation between "failure" and "flow" behavior. "Failure" behavior is represented by conventional SRP inelastic strainrange versus cyclic life relations, while "flow" behavior is captured in terms of the cyclic stress-strain response characteristics. Stress-strain response is calculated from simple equations developed from approximations to more complex cyclic constitutive models. For application to TMF life prediction, a new testing technique, bithermal cycling, is proposed as a means for generating the inelastic strainrange versus life relations. Flow relations for use in predicting TMF lives would normally be obtained from approximations to complex thermomechanical constitutive models. Bithermal flow testing is also proposed as an alternative to thermomechanical flow testing at low strainranges where the hysteresis loop is difficult to analyze. For the current paper, cyclic stress-strain response is calculated for the alloy 2-1/4Cr-1Mo steel in the post-weld, heat-treated condition for both thermomechanical and bithermal cycles and for a variety of strainranges and hold times. Bithermal failure behavior data are currently unavailable.

17. Key Words (Suggested by Author(s))	18. Distribution Statement
Fatique (metals); Low cycle fatigue; Thermomechanical fatigue; Life prediction; Creep-fatigue; Strainrange Partitioning constitutive modeling; Creep; Plasticity; Strain fatigue	Unclassified – Unlimited Subject Category 39

19. Security Classif. (of this report)	20. Security Classif. (of this page)	21. No of pages	22. Price*
Unclassified	Unclassified	24	A02

*For sale by the National Technical Information Service, Springfield, Virginia 22161